Shahid Chamran University of Ahvaz

Journal of Advanced Mathematical Modeling
ISSN (print): 2251-8088, ISSN (on-line): 2645-6141
Vol. 15 No. 2 (2025), pp. 87-112.
DOI: 10.22055/jamm.2025.47755.2303

FOURIER SPECTRAL APPROXIMATION FOR THE TIME-FRACTIONAL REACTION-DIFFUSION BRUSSELATOR SYSTEM

FARZANEH RAZAVI SOSAN, MEHDI GHASEMI AND MOJTABA FARDI*

Communicated by: Jalil Rashidinia

Abstract. This paper introduces a robust numerical method for analyzing the time-fractional reaction-diffusion Brusselator system. The problem is discretized in the spatial direction using the Fourier spectral method and in the temporal direction using a high-order approximation for the Caputo derivative. By leveraging the Fourier spectral method's properties, we can eliminate the second spatial derivatives from the system. The convergence of this method has been proven, and its efficiency and accuracy are demonstrated through various numerical examples. The findings reveal a consistent rate of convergence of two for multiple values of α, affirming the method's efficacy in tackling the established system.

1. Introduction

Fractional partial differential equations (FPDEs) are gaining widespread recognition as a powerful modeling tool in diverse fields of science and engineering [1, 2]. By incorporating fractional derivatives, FPDEs offer unparalleled insights into non-local and spatially heterogeneous phenomena, outperforming their integer-order counterparts. Applications of FPDEs span a wide range of disciplines, including hydrology, image denoising, finance, physics, biology, chemistry, and more. FPDEs accurately simulate fluid flow and

MSC(2020): 33C45; 65M70, 35R11.

Keywords: Time-Fractional; Caputo Derivative; Reaction-Diffiusion Brusselator System; Fourier Spectral Method.

Received: 14 August 2024, Accepted: 23 December 2025.

*Corresponding author.

solute transport in porous media, enhance image quality by removing noise while preserving essential features, and enable efficient pricing of complex financial instruments [3, 4, 5, 6, 7, 8, 9, 10]. The versatility and effectiveness of FPDEs have led to their growing adoption as a valuable tool for modeling non-local and heterogeneous phenomena across a wide spectrum of disciplines. FPDEs provide deeper insights and enhance our understanding of complex systems, making them an essential tool for researchers and practitioners alike [11, 12].

The reaction-diffusion Brusselator system (RDBS) is a mathematical model used to describe a type of chemical oscillator and pattern formation in reaction-diffusion systems. The Brusselator is named after Brussels, where the model was first introduced. It is a set of nonlinear differential equations that represent the dynamics of two chemical species interacting through reactions and diffusion. This model is particularly significant in the study of Turing patterns, which are spatial patterns that emerge spontaneously in reaction-diffusion systems. The Brusselator system has applications in various fields, including chemistry, biology, and physics, where it is used to model phenomena such as chemical waves, morphogenesis, and the formation of spatial structures in biological systems [13, 14].

The time-fractional RDBS (TFRDBS) is an extension of the classical Brusselator model, incorporating time-fractional derivatives to account for memory effects and anomalous diffusion processes. In this system, the time derivative in the governing equations is replaced with a fractional derivative, which allows for a more accurate description of processes where the rate of diffusion or reaction is not constant over time, such as in heterogeneous or complex media. This model is particularly useful in fields like biology and materials science, where anomalous diffusion and long-range temporal correlations play a critical role, such as in the spread of biological species, signal transmission in neurons, and the formation of patterns in heterogeneous materials [15]. In this paper, we investigate the TFRDBS described by:

$$
\begin{cases}
D^{\alpha}_{[0,t]}\phi - \lambda_1 + (\lambda_2+1)\phi - \phi^2\psi - \lambda_3\frac{\partial^2\phi}{\partial x^2} = f_1(x,t),\ x\in\mathbb{R},\ t>0,\\
D^{\alpha}_{[0,t]}\psi - \lambda_2\phi + \phi^2\psi - \lambda_3\frac{\partial^2\psi}{\partial x^2} = f_2(x,t),\ x\in\mathbb{R},\ t>0,\\
\phi(x,t) = \phi(x+2\pi,t),\ x\in\mathbb{R},\ t\geq 0,\\
\psi(x,t) = \psi(x+2\pi,t),\ x\in\mathbb{R},\ t\geq 0,
\end{cases}
\tag{1.1}
$$

where λ_1, λ_2 are the input chemicals and ϕ, ψ are the intermediate species.
The initial conditions for system (1.1) are given by

$$\phi(x,0) = \phi(x+2\pi,0) = \phi_0(x),\ x \in \mathbb{R}, \tag{1.2}$$

$$\psi(x,0) = \psi(x+2\pi,0) = \psi_0(x),\ x \in \mathbb{R}. \tag{1.3}$$

The time-fractional derivative in the system (1.1) is the Caputo fractional derivative (CFD) with order $0 < \alpha < 1$, and it is defined as

$$D^{\alpha}_{[0,t]}\phi(t) = \frac{1}{\Gamma(1-\alpha)} \int_0^t \frac{\partial \phi(\eta)}{\partial \eta}(t-\eta)^{-\alpha} d\eta, \tag{1.4}$$

where $\Gamma(\cdot)$ denotes the usual gamma function.

The motivation for employing the fractional form of the reaction-diffusion Brusselator system lies in its capability to capture memory effects and anomalous diffusion processes, which are prevalent in real-world phenomena such as biological pattern formation, chemical reactions, and material sciences. Traditional integer-order models often fail to accurately represent these long-range temporal correlations. By incorporating the Caputo fractional derivative, our approach provides a more flexible and precise description of diffusion and reaction dynamics. Furthermore, the combination of the Fourier spectral method with a high-order approximation for the fractional derivative enhances both accuracy and computational efficiency compared to classical finite difference and finite element methods, making it an effective choice for solving the TFRDBS.

Several studies have investigated the fractional BRDS using various analytical and numerical approaches. Jena et al. [16] employed the fractional reduced differential transform method (FRDTM) to obtain semi-analytical solutions and conducted a convergence analysis. Singh et al. [17] introduced the q-homotopy analysis transform method (q-HATM), demonstrating its computational efficiency for nonlinear fractional differential equations. Nisar et al. [18] applied the residual power series method (RPSM) to derive analytical solutions and analyzed them graphically. Recently, Singh et al. [19] proposed an innovative Vieta-Fibonacci wavelet collocation method, showing its effectiveness in solving the three-component fractional Brusselator system with high accuracy and computational efficiency. The present work builds upon these contributions by utilizing the Fourier spectral method for spatial discretization and a high-order approximation for the Caputo derivative, providing a robust and efficient numerical approach for solving TFRDBS.

Spectral methods are numerical techniques widely used for solving PDEs and FPDEs. These methods rely on representing the solution of the PDE or FPDE as a sum of basis functions, typically orthogonal polynomials or trigonometric functions [20, 21, 22, 23, 24, 25, 26]. One major advantage of the spectral method is its ability to converge when dealing with smooth solutions rapidly. However, the limited regularity of solutions to these problems, often due to constraints, makes achieving spectral accuracy challenging. The main objective of this study is to introduce a rapid approach for achieving a numerical solution to the TFRDBS by employing the Fourier spectral method. Utilizing the Fourier spectral method for spatial discretization of the TFRDBS, we showcase its efficacy in solving the system. This paper makes two key contributions. Firstly, we leverage the Fourier transform to simplify the TFRDBS into an ordinary differential equation (ODE) in frequency space. Subsequently, we employ an approximation for the Caputo derivative to solve the resultant ODE. Secondly, we perform a convergence analysis of the proposed method.

The structure of this paper is as follows: Section 2 outlines the application of Fourier spatial discretization to the TFRDBS. In Section 3, we furnish a convergence proof for the proposed methodology. Section 4 is devoted to presenting our numerical experiments' results, demonstrating the numerical technique's effectiveness. Finally, Section 5 offers concluding remarks.

2. The Numerical Method

2.1. **Fourier Spectral Approximation.** We'll employ the Fourier spectral method to solve equation (1.1)-(1.3). This method consists of expressing the function $\phi \in L^2(J)$, $J := (0, 2\pi)$ subject to periodic boundary conditions (PBCs) using its Fourier series representation as follows:

$$\phi(x) \approx \mathcal{F}(\phi)(x) := \Sigma_{k=-\infty}^{\infty} \hat{\phi}_k \exp(ikx). \tag{2.1}$$

Here, k denotes the Fourier wavenumber, and $\{\hat{\phi}_k\}_{k=-\infty}^{\infty}$ represent the Fourier coefficients, which can be computed using the formula:

$$\hat{\phi}_k = \int_0^{2\pi} (2\pi)^{-1} \exp(-ikx)\phi(x)dx. \tag{2.2}$$

Consider that for any function $\phi \in L^2(J)$ that is continuous, periodic and exhibits bounded variation on $\overline{J}$, the truncated series $\mathcal{P}_N(\phi) := \Sigma_{k=-N}^{N} \hat{\phi}_k \exp(ikx)$ converges uniformly to ϕ.

Next, let's define the points $x_j = j\frac{2\pi}{N},\ 0 \le j \le N-1$. We can then introduce the discrete Fourier transform (DFT):

$$\tilde{\phi}_k := \frac{1}{NA_k} \Sigma_{j=0}^{N-1} \phi_j \exp(-ikx_j),\ k = -\frac{N}{2} : \frac{N}{2}. \tag{2.3}$$

Here, $A_k = 1$ when $|k| < N/2$ and $A_k = 2$ when $|k| = N/2$. The definition of the DFT is:

$$\phi_j := \Sigma_{k=-\frac{N}{2}}^{\frac{N}{2}} \tilde{\phi}_k \exp(ikx_j),\ j = 0 : N-1. \tag{2.4}$$

We contemplate the space $\mathcal{X}_N := \mathcal{SPAN}\{\exp(ikx) : k = -N : N\}$ and $\mathcal{X} = \lim_{N\to\infty} \mathcal{X}_N$. In the context of the fractional Sobolev space, assuming $\phi \in H_p^m$ where $m \ge 2$, the semi-norm and norm of $H_p^m(J)$ can be expressed by:

$$\|\phi\|_m = (\Sigma_{k=-\infty}^{\infty}(1+k^2)^m|\tilde{\phi}_k|^2)^{\frac{1}{2}}, \qquad |\phi|_m = (\Sigma_{k=-\infty}^{\infty}|k|^{2m}|\tilde{\phi}_k|^2)^{\frac{1}{2}}. \tag{2.5}$$

The inner product of ϕ and ϱ in H_p^m is given by:

$$\langle \phi, \varrho \rangle := \Sigma_{k=-\infty}^{\infty}(1+k^2)^m \bar{\varrho}_k \phi_k.$$

Then, the standard weak formulation for (1.1) is to find ϕ and ψ in $\mathcal{X}$ such that

$$\begin{cases} \langle D_{[0,t]}^{\alpha}\phi, \varrho\rangle = \langle \lambda_1 - (\lambda_2+1)\phi, \varrho\rangle + \langle \phi^2\psi, \varrho\rangle + \lambda_3\langle \frac{\partial^2\phi}{\partial x^2}, \varrho\rangle + \langle f_1, \varrho\rangle, \\ \langle D_{[0,t]}^{\alpha}\psi, \varrho\rangle = \lambda_2\langle \phi, \varrho\rangle - \langle \phi^2\psi, \varrho\rangle + \lambda_3\langle \frac{\partial^2\phi}{\partial x^2}, \varrho\rangle + \langle f_2, \varrho\rangle, \\ \langle \phi(x,0), \varrho\rangle = \langle \phi_0, \varrho\rangle, \quad \langle \psi(x,0), \varrho\rangle = \langle \psi_0, \varrho\rangle, \quad \forall \varrho \in \mathcal{X}. \end{cases} \tag{2.6}$$

Approximation scheme: We find $\phi_N, \psi_N \in \mathcal{X}_N$ such that:

$$\begin{cases} \langle D_{[0,t]}^{\alpha}\phi_N, \varrho\rangle = \langle \lambda_1 - (\lambda_2+1)\phi_N, \varrho\rangle + \langle \phi_N^2\psi_N, \varrho\rangle + \lambda_3\langle \frac{\partial^2\phi_N}{\partial x^2}, \varrho\rangle + \langle f_1, \varrho\rangle, \\ \langle D_{[0,t]}^{\alpha}\psi_N, \varrho\rangle = \lambda_2\langle \phi_N, \varrho\rangle - \langle \phi_N^2\psi_N, \varrho\rangle + \lambda_3\langle \frac{\partial^2\phi_N}{\partial x^2}, \varrho\rangle + \langle f_2, \varrho\rangle, \\ \langle \phi_N(x,0), \varrho\rangle = \langle \phi_0, \varrho\rangle, \quad \langle \psi_N(x,0), \varrho\rangle = \langle \psi_0, \varrho\rangle, \quad \forall \varrho \in \mathcal{X}. \end{cases} \tag{2.7}$$

Taking the inner product of equation (2.7) with $\varrho = e^{ikx}$, and applying (2.3), we obtain:

$$\begin{cases} D_{[0,t]}^{\alpha}\tilde{\phi}_k(t) = \lambda_1 - (\lambda_2+1)\tilde{\phi}_k(t) + \mathcal{F}(\mathcal{F}^{-1}(\tilde{\phi}_k(t))^2.\mathcal{F}^{-1}(\tilde{\psi}_k(t))) - \lambda_3 k^2\tilde{\phi}_k(t) + \tilde{f}_1(t), \\ D_{[0,t]}^{\alpha}\tilde{\psi}_k(t) = \lambda_2\tilde{\psi}_k(t) - \mathcal{F}(\mathcal{F}^{-1}(\tilde{\phi}_k(t))^2.\mathcal{F}^{-1}(\tilde{\psi}_k(t))) - \lambda_3 k^2\tilde{\psi}_k(t) + \tilde{f}_2(t), \end{cases} \tag{2.8}$$

The initial conditions are given by

$$\tilde{\phi}(x,0) = \tilde{\phi}_0(x), \quad \tilde{\psi}(x,0) = \tilde{\psi}_0(x), \quad x_r \le x \le x_m.$$

Suppose that $\phi_j(t), \psi_j(t) \in L^2(0,T)$ for each spatial grid point x_j. Then, for each wave number k, the corresponding discrete Fourier coefficient $\tilde{\phi}_k(t)$ and $\tilde{\psi}_k(t)$ also belong to $L^2(0,T)$.

2.2. **Discretization of the Temporal Direction.** Given positive values M and even N, consider $t_n = ndt$ and $x_j = a + jh$ with $dt = T/M$, $h = (b-a)/N$ represent the temporal and spatial step sizes, respectively. The L1-2-3 formula, detailed in [27], provides an approximation for the CFD of order α with $0 < \alpha < 1$ and an accuracy of $4 - \alpha$. This formula is applicable when ϕ belongs to $C^4[0, t_n]$ and is expressed as:

$$\tilde{\mathcal{D}}^{\alpha}_{t_n}\phi(t)\Big|_{t=t_n} = \frac{dt^{-\alpha}}{\Gamma(2-\alpha)}(\delta^{\alpha}_0\phi_n - \Sigma_{j=1}^{n-1}(\delta^{\alpha}_{n-j-1} - \delta^{\alpha}_{n-j})\phi_j - \delta^{\alpha}_{n-1}\phi_0), \tag{2.9}$$

where the coefficients are defined as follows:
For $n = 1$, we have

$$\delta^{\alpha}_0 = 1;$$

For $n = 2$, we have

$$\delta^{\alpha}_0 = a^{\alpha}_0 + b^{\alpha}_0, \delta^{\alpha}_1 = a^{\alpha}_1 - b^{\alpha}_0;$$

For $n = 3$, we have

$$\delta^{\alpha}_l = \begin{cases} a^{\alpha}_l + b^{\alpha}_l + \omega^{\alpha}_l, & l = 0, \\ a^{\alpha}_l + b^{\alpha}_l - b^{\alpha}_{l-1} - 2\omega^{\alpha}_{l-1}, & l = 1, \\ a^{\alpha}_l - b^{\alpha}_{l-1} + \omega^{\alpha}_{l-2}, & l = 2, \end{cases}$$

For $n \geq 4$, we have

$$\delta^{\alpha}_l = \begin{cases} a^{\alpha}_l + b^{\alpha}_l + \omega^{\alpha}_l, & l = 0, \\ a^{\alpha}_l + b^{\alpha}_l - b^{\alpha}_{l-1} + \omega^{\alpha}_l - 2\omega^{\alpha}_{l-1}, & l = 1, \\ a^{\alpha}_l + b^{\alpha}_l - b^{\alpha}_{l-1} + \omega^{\alpha}_l - 2\omega^{\alpha}_{l-1} + \omega^{\alpha}_{l-2}, & l = 2 : n-3, \\ a^{\alpha}_l + b^{\alpha}_l - b^{\alpha}_{l-1} - 2\omega^{\alpha}_{l-1} + \omega^{\alpha}_{l-2}, & l = n-2, \\ a^{\alpha}_l - b^{\alpha}_{l-1} + \omega^{\alpha}_{l-2}, & l = n-1, \end{cases}$$

where

$$\begin{aligned} a_l^\alpha &= (l+1)^{1-\alpha} - l^{1-\alpha},\ 0 \le l \le n-1, \\ b_l^\alpha &= \tfrac{1}{2-\boldsymbol{\alpha}}[(l+1)^{2-\alpha} - l^{2-\alpha}] - \tfrac{1}{2}[(l+1)^{1-\alpha} + l^{1-\alpha}],\ l \ge 0, \\ \omega_l^\alpha &= -(\tfrac{1}{6}((l+1)^{1-\alpha} + 2l^{1-\alpha}) + \tfrac{1}{2-\alpha} l^{2-\alpha} - \tfrac{1}{(2-\alpha)(3-\alpha)}((l+1)^{3-\alpha} - l^{3-\alpha})),\ l \ge 0. \end{aligned}$$

By applying (2.8) and (2.9), we obtain the following system of equations:

$$(2.10)\quad \begin{cases} (\frac{dt^{-\alpha}}{\Gamma(2-\alpha)}\delta_0^\alpha + \lambda_3 k^2 + \lambda_2 + 1)\tilde{\phi}_{k,n+1} = \lambda_1 \\ +\frac{dt^{-\alpha}}{\Gamma(2-\alpha)}(\Sigma_{j=1}^n(\delta_{n-j}^\alpha - \delta_{n-j+1}^\alpha)\tilde{\phi}_{k,j} - \delta_n^\alpha \tilde{\phi}_{k,0}) \\ \qquad\qquad +\mathcal{F}(\mathcal{F}^{-1}(\tilde{\phi}_{k,n})^2 . \mathcal{F}^{-1}(\tilde{\psi}_{k,n})) + \tilde{f}_1(t_{n+1}), \\ (\frac{dt^{-\alpha}}{\Gamma(2-\alpha)}\delta_0^\alpha + \lambda_3 k^2 - \lambda_2)\tilde{\psi}_{k,n+1} \\ = \frac{dt^{-\alpha}}{\Gamma(2-\alpha)}(\Sigma_{j=1}^n(\delta_{n-j}^\alpha - \delta_{n-j+1}^\alpha)\tilde{\psi}_{k,j} - \delta_n^\alpha \tilde{\psi}_{k,0}) \\ \qquad\qquad +\mathcal{F}(\mathcal{F}^{-1}(\tilde{\phi}_{k,n})^2 . \mathcal{F}^{-1}(\tilde{\psi}_{k,n})) + \tilde{f}_2(t_{n+1}). \end{cases}$$

Here, $\tilde{\phi}_{k,n} := \frac{1}{NA_k}\sum_{j=0}^{N-1}\phi_j(t_n)\exp(-ikx_j), k = -\frac{N}{2} : \frac{N}{2}$, and $\tilde{\psi}_{k,n}$ is defined similarly.

3. Theoretical Analysis

Theorem 3.1. *(See [28]) For $\phi \in H_p^m$, $m \ge 2$ and $m \ge \rho \ge 0$, we get*

$$\|\phi - \mathcal{P}_N\phi\|_\rho \le N^{\rho-m}|\phi|_m,$$

where $\mathcal{P}_N(\phi) := \Sigma_{k=-N}^N \hat{\phi}_k \exp(ikx)$.

Theorem 3.2. *Let $\phi, \psi \in L^2(0,T;H_p^m)(m \ge 2)$ be solutions to (2.6), and let ϕ_N, ψ_N be solutions to (2.7), it follows*

$$\|\phi(t) - \phi_N(t)\| \le CN^{\rho-m},\ \|\psi(t) - \psi_N(t)\| \le CN^{\rho-m}$$

Proof. Let $e_N(t_n) = \phi_N(t_n) - \mathcal{P}_N\phi(t_n), \epsilon_N(t_n) = \psi_N(t_n) - \mathcal{P}_N\psi(t_n),\ n = 0, 1, .., M.$ We substitute $\mathcal{P}N\phi(t_n)$ and $\mathcal{P}N\psi(t_n)$ for $\phi_N(t_n)$ and $\psi_N(t_n)$ in (2.7), therefore we get

$$\begin{cases} \langle \frac{\partial^\alpha e_N(t)}{\partial t^\alpha}\Big|_{t=t_n}, \varrho\rangle = -(\lambda_2+1)\langle e_N, \varrho\rangle + \langle \phi_N^2\psi_N - \mathcal{P}_N\phi^2\mathcal{P}_N\psi, \varrho\rangle + \lambda_3\langle \frac{\partial^2 e_N(t_n)}{\partial x^2}, \varrho\rangle, \\ \langle \frac{\partial^\alpha \epsilon_N(t)}{\partial t^\alpha}\Big|_{t=t_n}, \varrho\rangle = \lambda_2\langle \epsilon_N, \varrho\rangle - \langle \phi_N^2\psi_N - \mathcal{P}_N\phi^2\mathcal{P}_N\psi, \varrho\rangle + \lambda_3\langle \frac{\partial^2 \epsilon_N(t_n)}{\partial x^2}, \varrho\rangle,\ \forall \varrho \in \mathcal{X}_N. \end{cases}$$

We put $\varrho = e_N(t_n)$ and apply the Caputo approximation defined by (2.9). Then we have

$$\begin{aligned} &\frac{dt^{-\alpha}}{\Gamma(2-\alpha)}(\delta_0^\alpha\langle e_N(t_n), e_N(t_n)\rangle - \Sigma_{j=1}^{n-1}(\delta_{n-j-1}^\alpha - \delta_{n-j}^\alpha)\langle e_N(t_j), e_N(t_n)\rangle - \delta_{n-1}^\alpha\langle e_N(t_0), e_N(t_n)\rangle) \\ &\quad = -(\lambda_2+1)\langle e_N(t_n), e_N(t_n)\rangle + \langle \phi_N^2\psi_N - \mathcal{P}_N\phi^2\mathcal{P}_N\psi, e_N(t_n)\rangle + \lambda_3\langle \frac{\partial^2 e_N(t_n)}{\partial x^2}, e_N(t_n)\rangle. \end{aligned}$$

Also we have

$$\begin{aligned}\langle\phi_N^2\psi_N &- \mathcal{P}_N\phi^2\mathcal{P}_N\psi, e_N(t_n)\rangle \leq \langle\phi_N^2\psi_N - \mathcal{P}_N\phi^2\psi_N, e_N(t_n)\rangle\\ &+ \langle\mathcal{P}_N\phi^2\psi_N - \mathcal{P}_N\phi^2\mathcal{P}_N\psi, e_N(t_n)\rangle\\ &\leq \|e_N(t_n)\|\|\phi_N^2 - \mathcal{P}_N\phi^2\|\|\psi_N\| + \|\mathcal{P}_N\phi^2\|\|\epsilon_N(t_n)\|\|e_N(t_n)\|. \end{aligned} \tag{3.1}$$

Therefore

$$\begin{aligned}(\frac{dt^{-\alpha}}{\Gamma(2-\alpha)}\delta_0^\alpha + \lambda_2 + 1)\|e_N(t_n)\|^2 &\leq \|e_N(t_n)\|(\|\frac{\partial^2 e_N(t_n)}{\partial x^2}\|\\ &+ \|\mathcal{P}_N u^2\|\|\epsilon_N(t_n)\| + \|u_N^2 - \mathcal{P}_N u^2\|\|v_N\|\\ &+ \frac{dt^{-\alpha}}{\Gamma(2-\alpha)}\Big[\delta_{n-1}^\alpha\|e_N(t_0)\| + \Sigma_{j=1}^{n-1}(\delta_{n-j-1}^\alpha - \delta_{m-j}^\alpha)\|e_N(t_j)\|\Big]).\end{aligned}$$

In the next step, we put $\varrho = \epsilon_N(t_n)$ and use the equation (2.9). Then, using (3.1), we obtain:

$$\begin{aligned}(\frac{dt^{-\alpha}}{\Gamma(2-\alpha)}\delta_0^\alpha)\|\epsilon_N(t_n)\|^2 &\leq \|\epsilon_N(t_n)\|(\|\frac{\partial^2 \epsilon_N(t_n)}{\partial x^2}\|\\ &+ \|\mathcal{P}_N\phi^2\|\|\epsilon_N(t_n)\| + \|\phi_N^2 - \mathcal{P}_N\phi^2\|\|\psi_N\|\\ &+ \frac{dt^{-\alpha}}{\Gamma(2-\alpha)}\Big[\delta_{n-1}^\alpha\|\epsilon_N(t_0)\| + \Sigma_{j=1}^{n-1}(\delta_{n-j-1}^\alpha - \delta_{n-j}^\alpha)\|\epsilon_N(t_j)\|\Big]).\end{aligned}$$

Suppose that $n = 1$. Using $e_N(0) = 0$ and $\epsilon_N(0) = 0$, we have

$$\begin{aligned}(\frac{dt^{-\alpha}}{\Gamma(2-\alpha)}\delta_0^\alpha &+ \lambda_2 + 1)\|e_N(t_1)\| \leq \|\frac{\partial^2 e_N(t_1)}{\partial x^2}\|\\ &+ \|\mathcal{P}_N\phi^2\|\|\epsilon_N(t_1)\| + \|\phi_N^2 - \mathcal{P}_N\phi^2\|\|\psi_N\|,\end{aligned} \tag{3.2}$$

and

$$\begin{aligned}(\frac{dt^{-\alpha}}{\Gamma(2-\alpha)}\delta_0^\alpha)\|\epsilon_N(t_1)\| &\leq \|\frac{\partial^2 \epsilon_N(t_1)}{\partial x^2}\|\\ +\|\mathcal{P}_N\phi^2\|\|\epsilon_N(t_1)\| &+ \|\phi_N^2 - \mathcal{P}_N\phi^2\|\|\psi_N\|,\end{aligned} \tag{3.3}$$

where $\delta_0^\alpha > 0$.

Since $\phi, \psi \in C^4[0,1]$, the right-hand side of equations (3.2) and (3.3) are bounded. By choosing a sufficiently small dt, we can conclude that $e_N(t_1) = 0$ and $\epsilon_N(t_1) = 0$.

By induction, we have $e_N(t_j) = 0$.

Then, we derive:

$$\begin{aligned}\|\phi(t)-\phi_N(t)\|^2 &\leq \|\phi(t)-\mathcal{P}_N\phi(t)\|^2+\|\mathcal{P}_N\phi(t)-\phi_N(t)\|^2\\ &\leq N^{2\rho-2m}|\phi(t)|_m^2+\|e_N(t)\|^2=N^{2\rho-2m}|\phi(t)|_m^2.\end{aligned}$$

Conversely, The quantity $|\phi(t)|_m^2$ remains bounded. So we can conclude that there is a constant C which $\|\phi(t)-\phi_N(t)\|\leq CN^{\rho-m}$. The same result can be achieved for ψ. □

Lemma 3.3. *(See [27]) Assume that $\phi\in C^4[0,T]$ and ${}_0^cD_t^\alpha\phi(t)=\tilde{\mathcal{D}}_t^\alpha\phi(t)+\mathcal{ER}(\phi(t))$. Then, we have*

$$\mathcal{ER}(\phi(t_1)) = \frac{-\alpha}{2\Gamma(1-\alpha)}\phi''(\theta_1)\int_{t_0}^{t_1}(r-t_0)(r-t_1)(t_1-r)^{-\alpha-1}dr,$$

$$\begin{aligned}\mathcal{ER}(\phi_k(t_2)) = &\frac{-\alpha}{\Gamma(1-\alpha)}(\frac{1}{2}\tilde{\phi}''(\theta_1)\int_{t_0}^{t_1}(r-t_0)(r-t_1)(t_2-r)^{-\alpha-1}dr\\ &+\frac{1}{6}\phi'''(\theta_2)\int_{t_1}^{t_2}(r-t_0)(r-t_1)(t_2-r)^{-\alpha}dr),\end{aligned}$$

and for $n\geq 3$, we have

$$\begin{aligned}\mathcal{ER}(\phi_k(t_n)) = &\frac{-\alpha}{\Gamma(1-\alpha)}(\frac{1}{2}\phi''(\theta_1)\int_{t_0}^{t_1}(r-t_0)(r-t_1)(t_n-r)^{-\alpha-1}dr\\ &+\frac{1}{6}\phi'''(\theta_2)\int_{t_1}^{t_2}(r-t_0)(r-t_1)(r-t_2)(t_n-r)^{-\alpha-1}dr\\ &+\frac{1}{4!}|\phi^{(4)}(\theta)|\Sigma_{j=3}^{n-1}\int_{t_{j-1}}^{t_j}\prod_{i=0}^{3}(r-t_{j-i})(t_n-r)^{-\alpha-1}dr\\ &-\frac{1}{4!}\phi^{(4)}(\theta_4)\int_{t_{n-1}}^{t_n}\prod_{i=1}^{3}(r-t_{n-i})(t_n-r)^{-\alpha}dr,\end{aligned}$$

in which

$$\begin{aligned}&\theta_1\in(t_0,t_1),\ \theta_2\in(t_1,t_2),\\ &\theta\in(t_2,t_{n-1}),\ \theta_4\in(t_{n-1},t_n).\end{aligned}$$

Remark 3.4. Let ${}_0^cDt_k{}^{m*\alpha}\tilde{\phi}_k(t)$ denote the m-th time CFD of $\tilde{\phi}_k(t)$, defined as

$${}_0^cDt_k{}^\alpha({}_0^cDt_k{}^\alpha({}_0^cDt_k{}^\alpha(\ldots(\tilde{\phi}_k(t))).$$

By leveraging Lemma 3.3 and the properties of CFDs, we can derive:

$$ {}_0^cD_{t_k}^{m*\alpha}\tilde{\phi}_k(t) = \tilde{\mathcal{D}}_{t_k}^{m*\alpha}\tilde{\phi}_k(t) + \Sigma_{s=1}^{m-1}{}_0^cD_{t_k}^{s*\alpha}\mathcal{ER}_{\tilde{\mathcal{D}}_{t_k}^{(m-s-1)*\alpha}\tilde{\phi}_k}(t) + \mathcal{ER}_{\tilde{\mathcal{D}}_{t_k}^{(m-1)*\alpha}\tilde{\phi}_k}(t). \tag{3.4} $$

Theorem 3.5. *Suppose $\phi \in C^4[0,T]$. For any $t_j, t_n \in [0,T]$ the following relation holds*

$$ |{}_0^cD_{t_j}^{m*\alpha}\mathcal{ER}(\tilde{\phi}_k(t_n))| = \mathcal{O}(dt^{2-(m+1)\alpha}), \tag{3.5} $$

Proof. By considering Lemma 3.3 and Remark 3.4, we can achieve the following formulas

$$ \begin{aligned}
{}_0^cD_{t_1}^{\alpha}\mathcal{ER}(\tilde{\phi}_k(\psi)) &= \frac{\alpha}{2\Gamma(-\alpha+1)}\tilde{\phi}''(\theta_1)\int_{t_0}^{t_1}\Big(\int_{t_0}^{v}(r-t_0)(v-r)^{-\alpha}dr\Big)'(t_1-v)^{-\alpha}dv \\
&= \frac{-\alpha^2}{2\Gamma^2(-\alpha+1)}\tilde{\phi}''(\theta_1)\int_{t_0}^{t_1}\Big(\int_{t_0}^{v}(r-t_0)(v-r)^{-\alpha-1}dr\Big)(t_1-v)^{-\alpha}dv \\
&= \frac{-\alpha^2}{2\Gamma^2(-\alpha+1)}\tilde{\phi}''(\theta_1)\int_{t_0}^{t_1}(r-t_0)\Big(\int_{s}^{t_1}(v-r)^{-\alpha-1}(t_1-v)^{-\alpha}dv\Big)dr \\
&= \frac{-\alpha^2}{2\Gamma^2(-\alpha+1)}\tilde{\phi}''(\theta_1)\int_{t_0}^{t_1}(r-t_0)(t_1-r)^{-2\alpha}dr\int_0^1 q^{-\alpha-1}(1-q)^{-\alpha}dq \\
&= \frac{-\alpha^2\Gamma(-\alpha)}{2\Gamma(-2\alpha+1)\Gamma(-\alpha+1)}\tilde{\phi}''(\theta_1)\int_{t_0}^{t_1}(r-t_0)(t_1-r)^{-2\alpha}dr, \\
&= \frac{\alpha}{2\Gamma(-2\alpha+1)}\tilde{\phi}''(\theta_1)\int_{t_0}^{t_1}(r-t_0)(t_1-r)^{-2\alpha}dr.
\end{aligned} $$

In the same manner, we can demonstrate

$$ {}_0^cD_{t_1}^{m*\alpha}\mathcal{ER}(\tilde{\phi}_k) = \frac{\alpha}{2\Gamma(-(m+1)\alpha+1)}\tilde{\phi}''(\theta_1)\int_{t_0}^{t_1}(r-t_0)(t_1-r)^{-(m+1)\alpha}dr. $$

Therefore

$$ |{}_0^cD_{t_1}^{m*\alpha}\mathcal{ER}(\tilde{\phi}_k)| \le |\frac{\alpha}{2\Gamma(-(m+1)\alpha+2)}|\max_{t_0\le t\le t_1}|\tilde{\phi}_k''(t)|dt^{2-(m+1)\alpha}. \tag{3.6} $$

Also, we have

$$ \begin{aligned}
|{}_0^cD_{t_2}^{\alpha}\mathcal{ER}(\tilde{\phi}_k(v))| \le \Bigg|&\frac{\alpha}{\Gamma^2(1-\alpha)}\int_{t_0}^{t_2}\Bigg[\frac{\alpha+1}{2}\tilde{\phi}''(\theta_1)\int_{t_0}^{t_1}(r-t_0)(r-t_1)(v-r)^{-\alpha-2}dr \\
&+\frac{\alpha}{6}\tilde{\phi}'''(\theta_2)\int_{t_1}^{v}(r-t_0)(r-t_1)(v-r)^{-\alpha-1}dr\Bigg](t_2-v)^{-\alpha}dv\Bigg|.
\end{aligned} $$

Since the time step is less than one, we have $t_1 \le r \le v \le 1$ and $(v-r)^{-1} > 1$. Then

$$\begin{aligned}
\left|{}_0^cD_{t_2}^{\alpha}\mathcal{ER}(\tilde{\phi}_k)\right| &\le \left|\frac{\alpha(\alpha+1)}{\Gamma^2(-\alpha+1)}\int_{t_0}^{t_2}(\int_{t_0}^{v}\mathcal{H}(r)(v-r)^{-\alpha-2}dr)(t_2-v)^{-\alpha}dv\right|,\\
&= \left|\frac{\alpha(\alpha+1)}{\Gamma^2(-\alpha+1)}\int_{t_0}^{t_2}\mathcal{H}(r)(\int_{r}^{t_2}(v-r)^{-\alpha-2}(t_2-v)^{-\alpha}dv)dr\right|,\\
&= \left|\frac{\alpha(\alpha+1)}{\Gamma^2(-\alpha+1)}\int_{t_0}^{t_2}\mathcal{H}(r)(t_2-r)^{-2\alpha-1}dr\int_{0}^{1}q^{-\alpha-2}(1-q)^{-\alpha}dq\right|,\\
&= \left|\frac{1}{\Gamma(-2\alpha)}\int_{t_0}^{t_2}\mathcal{H}(r)(t_2-r)^{-2\alpha-1}dr\right|,
\end{aligned}$$

where

$$\mathcal{H}(r) = \begin{cases} \frac{1}{2}\tilde{\phi}''(\theta_1)(r-t_0)(r-t_1), & t_0 \le r \le t_1,\\ \\ \frac{1}{6}\tilde{\phi}'''(\theta_2)(r-t_0)(t_1-r), & t_1 < r \le t_2. \end{cases}$$

In the same manner, we can demonstrate

$$|{}_0^cD_{t_2}^{m*\alpha}\mathcal{ER}(\tilde{\phi}_k)| \le \left|\frac{1}{\Gamma(-(m+1)\alpha)}\int_{t_0}^{t_2}\mathcal{H}(r)(t_2-r)^{-(1+(m+1)\alpha)}dr\right|.$$

Therefore

$$\begin{aligned}
|{}_0^cD_{t_2}^{m*\alpha}\mathcal{ER}(\tilde{\phi}_k)| &\le |\frac{1}{\Gamma(-(m+1)\alpha)}|(\frac{1}{2}\tilde{\phi}''(\theta_1)\int_{t_0}^{t_1}(r-t_0)(t_1-r)(t_2-r)^{-(m+1)\alpha-1}dr\\
&\quad +\frac{1}{6}\tilde{\phi}'''(\theta_2)\int_{t_1}^{t_2}(r-t_0)(r-t_1)(t_2-r)^{-(m+1)\alpha-1}dr) \qquad (3.7)\\
&\le |\frac{1}{\Gamma(-(m+1)\alpha+1)}|\left(\frac{1}{2}\max_{t_0\le t\le t_1}|\tilde{\phi}_k''(t)| + \frac{1}{3}\max_{t_1\le t\le t_2}|\tilde{\phi}_k'''(t)|\right)dt^{2-(m+1)\alpha}.
\end{aligned}$$

Moreover

$$|{}_0^cD_{t_n}^{m*\alpha}\mathcal{ER}(\tilde{\phi}_k(v))| \le \left|\frac{1}{\Gamma(-(m+1)\alpha)}\int_{t_0}^{t_n}\mathcal{L}(r)(t_n-r)^{-(m+1)\alpha-1}dr\right|,$$

where

$$\mathcal{L}(r)=\begin{cases}\frac{-\tilde{\phi}''(\theta_1)}{2}(t_0-r)(t_1-r), & t_0\le r\le t_1,\\ \frac{\tilde{\phi}'''(\theta_2)}{6}(t_0-r)(t_1-r)(t_2-r), & t_1<r\le t_2,\\ \frac{-\tilde{\phi}^{(4)}(\theta)}{4!}\prod_{i=0}^{3}(t_{j-i}-r), & t_{j-1}<r\le t_j,\\ \frac{\tilde{\phi}^{(4)}(\theta_4)}{4!}\prod_{i=1}^{3}(r-t_{n-i}), & t_{n-1}<r\le t_n.\end{cases}\qquad j=3:n-1,$$

Therefore

$$\begin{aligned}\left|{}_0^cD_{t_n}^{m*\alpha}\mathcal{ER}(\tilde{\phi}_k)\right| \;\le\; & \left|\frac{1}{\Gamma(-(m+1)\alpha)}\right|\Big(\left|\frac{1}{2}\tilde{\phi}''(\theta_1)\int_{t_0}^{t_1}(r-t_0)(t_1-r)(t_n-r)^{-(m+1)\alpha-1}dr\right|\\ &+\left|\frac{1}{6}\tilde{\phi}'''(\theta_2)\int_{t_1}^{t_2}(r-t_0)(r-t_1)(t_2-r)(t_n-r)^{-(m+1)\alpha-1}dr\right|\\ &+\left|\frac{1}{4!}\tilde{\phi}^{(4)}(\theta)\Sigma_{j=3}^{n-1}\int_{t_{j-1}}^{t_j}\prod_{i=0}^{3}(r-t_{j-i})(t_n-r)^{-(m+1)\alpha-1}dr\right|\\ &+\left|\frac{1}{4!}\tilde{\phi}^{(4)}(\theta_4)\int_{t_{n-1}}^{t_n}\prod_{i=1}^{3}(r-t_{n-i})(t_n-r)^{-(m+1)\alpha-1}dr\right|\Big).\end{aligned}$$

So, we can write:

$$\begin{aligned}|{}_0^cD_{t_n}^{m*\alpha}\mathcal{ER}(\tilde{\phi}_k(t_n))| \;\le\; & \left|\frac{1}{\Gamma(-(m+1)\alpha+1)}\right|\Big(\frac{1}{2}\max_{t_0\le t\le t_1}|\tilde{\phi}_k''(t)|dt^{2-(m+1)\alpha}\\ &+\frac{1}{3}\max_{t_0\le t\le t_2}|\tilde{\phi}_k'''(t)|dt^{3-(m+1)\alpha}+\frac{1}{4}\max_{t_0\le t\le t_{n-1}}|\tilde{\phi}_k^{(4)}(t)|dt^{4-(m+1)\alpha}\\ &+\frac{1}{4}\max_{t_0\le t\le t_n}|\tilde{\phi}_k^{(4)}(t)|dt^{3-(m+1)\alpha}\Big).\end{aligned}$$

Then

$$|{}_0^cD_{t_j}^{m*\alpha}\mathcal{ER}(\tilde{\phi}_k(t_n))|\le\chi_{ji}dt^{2-(m+1)\alpha},\tag{3.8}$$

where

$$\chi_{ji}(\tilde{\phi}_k) = \begin{cases} |\frac{\alpha}{2\Gamma(-(m+1)\alpha+2)}| \max_{t_0\le t\le t_1} |\tilde{\phi}_k''(t)|, & j=1, \\ |\frac{1}{\Gamma(1-(m+1)\alpha)}|(\frac{1}{2}\max_{t_0\le t\le t_1}|\tilde{\phi}_k''(t)| + \frac{1}{3}\max_{t_1\le t\le t_2}|\tilde{\phi}_k'''(t)|), & j=2, \\ |\frac{1}{\Gamma(-(m+1)\alpha+1)}|(\frac{1}{2}\max_{t_0\le t\le t_1}|\tilde{\phi}_k''(t)| + \frac{dt}{3}\max_{t_0\le t\le t_2}|\tilde{\phi}_k'''(t)| \\ +\frac{dt^2}{4}\max_{t_0\le t\le t_{n-1}}|\tilde{\phi}_k^{(4)}(t)| + \frac{dt}{4}\max_{t_0\le t\le t_n}|\tilde{\phi}_k^{(4)}(t)|). & j=3,4,\cdots \end{cases}$$

□

Theorem 3.6. *Suppose that $\phi, \psi \in C^4[0,t_n]$ are the exact solutions of (1.1) And $\tilde{\phi}, \tilde{\psi}$, $\tilde{\phi}^c, \tilde{\psi}^c$ are approximate solutions of (2.8) by Eqs. (1.4) and (2.9). Then, we have:*

$$|e_{j,n}| = \mathcal{O}(dt^2),\ |\epsilon_{j,n}| = \mathcal{O}(dt^2).$$

where

$$e_{j,n} = \tilde{\phi}_j(t_n) - \tilde{\phi}_j^c(t_n),\ \epsilon_{j,n} = \tilde{\psi}_j(t_n) - \tilde{\psi}_j^c(t_n).$$

Proof. We replace (2.10) in (2.8) and consider Lemma (3.3), then obtain

$$|\hat{\phi}_{j,n} - \tilde{\phi}_{j,n}^c| \le \Sigma_{s=1}^{n-1} dt^{(n+1-s)\alpha} |{}_0^c D_{t_s}^{(n-s)*\alpha} \mathcal{ER}(\tilde{\phi}_j(t_s))| + dt^\alpha |\mathcal{ER}(\tilde{\phi}_j(t_n))|, \tag{3.9}$$

then by applying Theorem 3.5 for equation (3.9) we get $|e_{j,n}| = \mathcal{O}(dt^2)$. In the same way, we can show that $|\epsilon_{j,n}| = \mathcal{O}(dt^2)$. □

Theorem 3.7. *The proposed numerical method is consistent.*

Proof. We start with the expression:

$$\left(\frac{dt^{-\alpha}}{\Gamma(2-\alpha)}\delta_0^\alpha + \lambda_3 k^2 + \lambda_2 + 1\right)\tilde{\phi}_{k,n+1} = \frac{dt^{-\alpha}}{\Gamma(2-\alpha)}\left(\sum_{j=1}^{n-1}(\delta_{n-j-1}^\alpha + \delta_{n-j}^\alpha)\tilde{\phi}_{k,j} + \delta_{n-1}^\alpha \tilde{\phi}_{k,0}\right) + (\tilde{\phi^2\psi})_{k,n}.$$

By substituting Taylor expansions into the numerical scheme, we obtain:

$$\left(\frac{dt^{-\alpha}}{\Gamma(2-\alpha)}\delta_0^\alpha + \lambda_3 k^2 + \lambda_2 + 1\right)\tilde{\phi}_{k,n+1} = \frac{dt^{-\alpha}}{\Gamma(2-\alpha)}\Big(\delta_0^\alpha \tilde{\phi}_{k,n} + \Big(\sum_{j=0}^{n-1}\delta_j^\alpha - \delta_0^\alpha\Big)dt\tilde{\phi}_{k,j}' + \mathcal{O}(dt^2)\Big) + (\tilde{\phi^2\psi})_{k,n}.$$

Using $\sum_{j=0}^{n-1}\delta_j^\alpha = dt^{\alpha-1}$ from [27], the equation simplifies to:

$$\left(\frac{dt^{-\alpha}}{\Gamma(2-\alpha)}\delta_0^\alpha + \lambda_3 k^2 + \lambda_2 + 1\right)\tilde{\phi}_{k,n+1} = \frac{dt^{-\alpha}}{\Gamma(2-\alpha)}\left(\delta_0^\alpha\tilde{\phi}_{k,n} + dt^\alpha\tilde{\phi}'_{k,j} - \delta_0^\alpha dt\tilde{\phi}'_{k,j}\right) + (\widetilde{\phi^2\psi})_{k,n} + \mathcal{O}(dt).$$

Define $A = \frac{dt^{-\alpha}}{\Gamma(2-\alpha)}\delta_0^\alpha + \lambda_3 k^2 + \lambda_2 + 1$. The truncation error is $e_{n+1} = \tilde{\phi}(t_{n+1}) - \tilde{\phi}_{n+1}$. By Taylor expanding $\tilde{\phi}(t_{n+1})$:

$$e_{n+1} = \frac{1}{A}\Big(\frac{dt^{-\alpha}}{\Gamma(2-\alpha)}e_n + 2e_n\widetilde{(\phi(t)\psi)}_{k,n} + \widetilde{(\phi^2(t)\psi)}_{k,n} + e_n^2\tilde{\phi}_{k,n} - (\lambda_3 k^2 + \lambda_2 + 1)\tilde{\phi}(t_n) + dt^\alpha\tilde{\phi}'_{k,j} - \delta_0^\alpha dt\tilde{\phi}'_{k,j}\Big) + \mathcal{O}(dt).$$

Thus,

$$e_{n+1} = \frac{dt^{-\alpha}}{A\Gamma(2-\alpha)}e_n + \frac{1}{A}\Big(+ 2e_n\widetilde{(\phi(t)\psi)}_{k,n} + \widetilde{(\phi^2(t)\psi)}_{k,n} + e_n^2\tilde{\phi}_{k,n} - (\lambda_3 k^2 + \lambda_2 + 1)\tilde{\phi}(t_n) + dt^\alpha\tilde{\phi}'_{k,j} - \delta_0^\alpha dt\tilde{\phi}'_{k,j}\Big) + \mathcal{O}(dt).$$

Since $\frac{dt^{-\alpha}}{A\Gamma(2-\alpha)} < 1$, the truncation error e_{n+1} approaches zero as dt decreases. Therefore, we conclude that the numerical method is consistent. The proof for the second equation in the system is identical. □

Theorem 3.8. *The numerical method is stable if* $|\mathcal{M}_{k,n}| < \lambda_3 k^2 + \lambda_2 + 1$ *where* $\mathcal{M}_{k,n} = \widetilde{(\phi^2 + 2\phi\psi)}_{k,n}$.

Proof. Let E_0 denote the perturbation in the first step, and define $\mathcal{M}_{k,n} = \widetilde{(\phi^2 + 2\phi\psi)}_{k,n}$. Then we have

$$\left(\frac{dt^{-\alpha}}{\Gamma(2-\alpha)}\delta_0^\alpha + \lambda_3 k^2 + \lambda_2 + 1\right)E_{n+1} = \frac{dt^{-\alpha}}{\Gamma(2-\alpha)}\left(\sum_{j=1}^{n}(\delta_{n-j}^\alpha - \delta_{n-j+1}^\alpha)E_j + \delta_n^\alpha E_0\right) + \mathcal{M}_{k,n}E_n,$$

where $\delta_0^\alpha > \delta_2^\alpha > \cdots > \delta_n^\alpha > 0$ and $\delta_1 \in (-\frac{7}{6}, 1)$. Suppose $E_n = r^{n+1}$, with $|r| > 1$. When $\delta_1^\alpha > 0$, the equation reduces to:

$$\left(\frac{dt^{-\alpha}}{\Gamma(2-\alpha)}\delta_0^\alpha + \lambda_3 k^2 + \lambda_2 + 1\right)|r| \le \frac{dt^{-\alpha}}{\Gamma(2-\alpha)}\delta_0^\alpha + |\mathcal{M}_{k,n}|.$$

Since $|\mathcal{M}_{k,n}| < \lambda_3 k^2 + \lambda_2 + 1$, we deduce that $|r| < 1$, which leads to a contradiction with the initial assumption. We now turn to the case where $\delta_1^\alpha < 0$, from which we obtain:

$$\begin{aligned}\left(\frac{dt^{-\alpha}}{\Gamma(2-\alpha)}\delta_0^\alpha + \lambda_3 k^2 + \lambda_2 + 1\right)|E_{n+1}| &\leq \frac{dt^{-\alpha}}{\Gamma(2-\alpha)}\left(\sum_{j=1}^{n}(\delta_{n-j}^\alpha - \delta_{n-j+1}^\alpha)|E_j| + \delta_n^\alpha|E_0|\right) \\ &\quad + \mathcal{M}_{k,n}|E_n| + 2(\delta_2^\alpha - \delta_1^\alpha)|E_{n-1}|.\end{aligned}$$

Since $|\mathcal{M}_{k,n}| < \lambda_3 k^2 + \lambda_2 + 1$, we obtain

$$dt^{-\alpha}\tilde{\mathcal{D}}_{t_{n+1}}^\alpha |E_{n+1}| \leq 2(\delta_2^\alpha - \delta_1^\alpha)|E_{n-1}|.$$

Therefore, we conclude that

$$dt^{-\alpha}\ln(|r|)(n+1)^{1-\alpha}E_{1,2-\alpha}((n+1)\ln|r|) \leq 2(\delta_2^\alpha - \delta_1^\alpha)|r|^n,$$

where $E_{a,b}(z)$ denotes the Mittag-Leffler function.
It follows that

$$dt^{-\alpha}\ln(|r|)n^{\frac{1-\alpha}{2}}|r|^n \leq 2(\delta_2^\alpha - \delta_1^\alpha)|r|^n.$$

Therefore,

$$(dt\sqrt{n})^{-\alpha}\ln(|r|)\sqrt{n} \leq 2(\delta_2^\alpha - \delta_1^\alpha).$$

This leads to a contradiction when dt is sufficiently small. Therefore, the desired result holds. An analogous reasoning applies to the second equation of the system. □

4. **Numerical Examples**

We give three numerical examples to demonstrate the method's efficiency for TFRDBS. All the computations are carried out using Matlab 9.8.0 (R2020a). We measure the error by infinity norm and root mean square (RMS) errors:

$$E_{RMS} = (\frac{1}{M}\Sigma_{i=1}^{M}(\phi_{exact}(T) - \phi_{approx}(T))^2)^{\frac{1}{2}},$$
$$E_{RMS} = (\frac{1}{M}\Sigma_{i=1}^{M}(\psi_{exact}(T) - \psi_{approx}(T))^2)^{\frac{1}{2}},$$

and

$$\begin{aligned}E_\infty &= \|\phi_{exact}(T) - \phi_{approx}(T)\|_\infty, \\ E_\infty &= \|\psi_{exact}(T) - \psi_{approx}(T)\|_\infty.\end{aligned}$$

Example 4.1. *Consider the following TFRDBS*

$$\begin{cases} D^{\alpha}_{[0,t]}\phi = -1.3\phi + \phi^2\psi + \frac{\partial^2\phi}{\partial x^2} + f_1(x,t), \\ D^{\alpha}_{[0,t]}\psi = 0.3\phi - \phi^2\psi + \frac{\partial^2\psi}{\partial x^2} + f_2(x,t), \end{cases} \tag{4.1}$$

where $0 < \alpha < 1$, $0 \le t \le 1$ *and*

$$f_1(x,t) = \frac{\Gamma(1.9)}{\Gamma(1.9-\alpha)} t^{0.9-\alpha} \sin(2\pi x) + 1.3\sin(2\pi x) - \sin^2(2\pi x)\cos(2\pi x) + 4\pi^2 sin(2\pi x),$$

$$f_2(x,t) = \frac{\Gamma(1.9)}{\Gamma(1.9-\alpha)} t^{0.9-\alpha} \cos(2\pi x) - 0.3\sin(2\pi x) + \sin^2(2\pi x)\cos(2\pi x) + 4\pi^2\cos(2\pi x),$$

For (4.1), the following initial conditions are considered:

$$\phi(x,0) = sin(2\pi x), \psi(x,0) = cos(2\pi x).$$

The exact solutions of the above problem can be expressed as $\phi(x,t) = (t^{0.9})\sin(2\pi x)$ and $\psi(x,t) = (t^{0.9})\cos(2\pi x)$.

Please take the following information into consideration: Tables 1 and 2 show the convergence rate, the RMS, infinity norm error, and CPU time of ϕ and ψ for $0 \le \alpha \le 1$ with $N = 16$ and $dt = 0.1, 0.05, 0.025, 0.0125, 0.0063$, respectively. The numerical analysis results show that the proposed method's convergence rates closely approach 2 for $0 \le \alpha \le 1$. The numerical and exact solutions are compared in Figure 2 with $\alpha = 0.1, N = 32$ and $dt = 0.001$. Figure 3 shows the error for different dt and α with $N = 32$. Figure 5 depicts the error of ϕ and ψ for $N = 512$ and $\alpha = 0.05, dt = 0.002$.

Example 4.2. *Consider the following TFRDBS*

$$\begin{cases} D^{\alpha}_{[0,t]}\phi = -1.7\phi + \phi^2\psi + 0.1\frac{\partial^2\phi}{\partial x^2} + f_1(x,t), \\ D^{\alpha}_{[0,t]}\psi = 0.7\phi - \phi^2\psi + 0.1\frac{\partial^2\psi}{\partial x^2} + f_2(x,t), \end{cases} \tag{4.2}$$

where $0 < \alpha < 1$ *and* $0 \le t \le 1$. *The initial conditions are:*

$$\phi(x,0) = x^2(1-x)^2, \psi(x,0) = x^4(1-x)^4.$$

We choose $f_1(x,t)$ *and* $f_2(x,t)$ *so that the exact solutions of the system (4.2) are* $\phi(x,t) = t^{0.9}x^2(1-x)^2$ *and* $\psi(x,t) = t^{0.9}x^4(1-x)^4$.

In Figure 4, the comparison between the exact and numerical solutions of this example is illustrated for $\alpha = 0.5$ using $dt = 0.001$, and $N = 128$. Meanwhile, in Figure 5, the error is portrayed for $\alpha = 0.5$ using $dt = 0.01$, and $N = 1024$. Remarkably, the error

TABLE 1. The obtained results for ϕ using the proposed method when $N = 16$ in Example 1.

α	dt	E_∞	$C-R$	E_{RMS}	$CPU(s)$
0.1	0.1000	$7.30458166e{-7}$	–	$5.16607900e{-7}$	0.0078
	0.0500	$1.86881453e{-7}$	1.9667	$1.32169686e{-7}$	0.0114
	0.0250	$4.92599613e{-8}$	1.9236	$3.48385205e{-8}$	0.0196
	0.0125	$1.31276872e{-8}$	1.9078	$9.28439982e{-9}$	0.0443
	0.0063	$3.51490136e{-9}$	1.9011	$2.48587142e{-9}$	0.1075
0.3	0.1000	$1.39687251e{-6}$	–	$1.39687251e{-6}$	0.0074
	0.0500	$3.54779461e{-7}$	1.9772	$3.54779461e{-7}$	0.0105
	0.0250	$9.45386313e{-8}$	1.9079	$9.45386313e{-8}$	0.0199
	0.0125	$3.63212381e{-9}$	1.8798	$2.56877695e{-8}$	0.0441
	0.0063	$9.97790405e{-9}$	1.8640	$7.05675476e{-9}$	0.1037
0.5	0.1000	$2.85281251e{-6}$		$2.01762597e{-6}$	0.0058
	0.0500	$7.24873382e{-7}$	1.9766	$5.12659449e{-7}$	0.0090
	0.0250	$2.01649783e{-7}$	1.8459	$1.42614698e{-7}$	0.0197
	0.0125	$5.87724808e{-8}$	1.7786	$4.15662076e{-8}$	0.0398
	0.0063	$1.77471135e{-8}$	1.7276	$1.25514529e{-8}$	0.0878

remains minimal, underscoring the efficiency of the present method, as demonstrated in Figure 5. Additionally, Table 3 presents the convergence rate, the RMS, infinity norm error, and CPU time for $dt = 0.01$, $0 \leq \alpha \leq 1$, and various values of N.

Example 4.3. *Consider the following TFRDBS*

$$\begin{cases} D^{\alpha}_{[0,t]}\phi = 1 - 1.5\phi + \phi^2\psi + 0.002\frac{\partial^2\phi}{\partial x^2} + f_1(x,t), \\ D^{\alpha}_{[0,t]}\psi = 0.5\phi - \phi^2\psi + 0.002\frac{\partial^2\psi}{\partial x^2} + f_2(x,t), \end{cases} \tag{4.3}$$

where $0 < \alpha < 1$, $0 \leq t \leq 1$ *and For (4.1), the following initial conditions are considered:*

$$\phi(x,0) = e^{\sin(2\pi x)}, \psi(x,0) = e^{\cos(2\pi x)}.$$

In this example, we examine the Brusselator model, which is defined by several key parameters that significantly influence the dynamics of the chemical reactions taking place

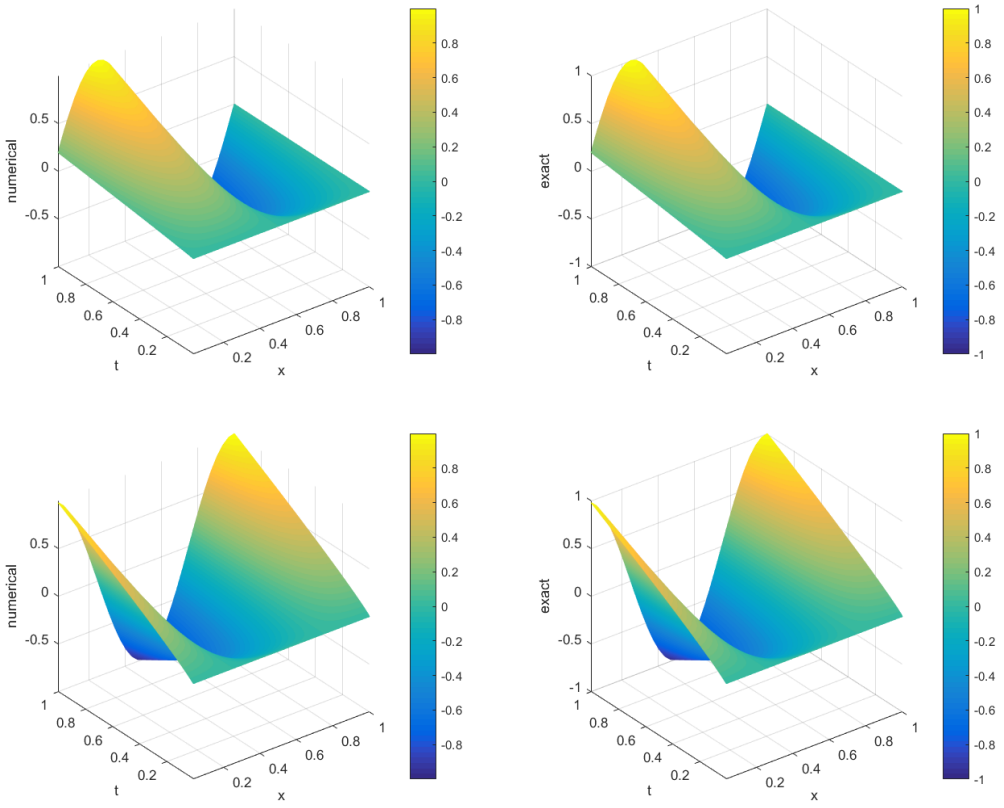


FIGURE 1. Exact and numerical solutions for ϕ (up) and ψ (down) for $\alpha = 0.1, N = 32$ and $dt = 0.001$ in Example 1.

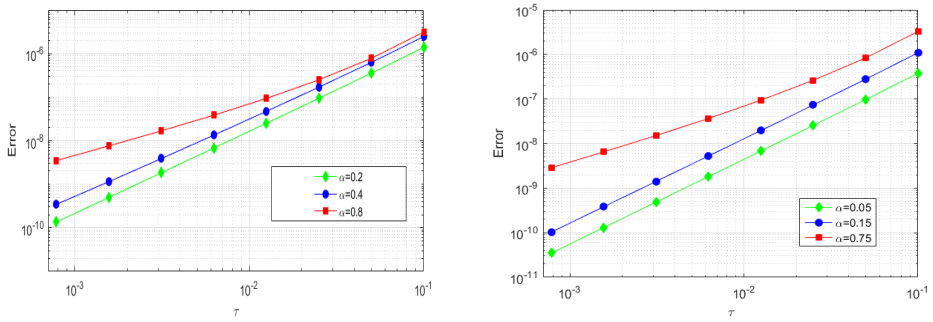


FIGURE 2. Infinity error for ϕ (left) and ψ (right) when $N = 16$ in Example 1.

within it. The parameter $\lambda_1 = 1$ represents the rate at which substance ψ is produced, typically expressed in moles per liter per second (mol/(L·s)). Conversely, $\lambda_2 = 0.5$ indicates the rate at which substance ψ is consumed in reactions. Additionally, λ_2 also

TABLE 2. The obtained results for ψ using the proposed method when $N = 16$ in Example 1.

α	dt	E_∞	$C-R$	E_{RMS}	$CPU(s)$
0.1	0.1000	$7.42078264e{-7}$	–	$5.23652646e{-7}$	0.0131
	0.0500	$1.89872644e{-7}$	1.9665	$1.33984985e{-7}$	0.0235
	0.0250	$5.00530056e{-8}$	1.9235	$3.53202700e{-8}$	0.0346
	0.0125	$1.33402906e{-8}$	1.9077	$9.41367583e{-9}$	0.0737
	0.0063	$3.57217999e{-9}$	1.9009	$2.52073552e{-9}$	0.1574
0.3	0.1000	$2.00990872e{-6}$	–	$1.41831216e{-6}$	0.0122
	0.0500	$5.10783350e{-7}$	1.9763	$3.60440124e{-7}$	0.0235
	0.0250	$1.36196464e{-7}$	1.9070	$9.61087949e{-8}$	0.0342
	0.0125	$3.70340237e{-8}$	1.8788	$2.61335972e{-8}$	0.0735
	0.0063	$1.01823252e{-8}$	1.8628	$7.18532440e{-9}$	0.1491
0.5	0.1000	$2.91129813e{-6}$		$2.05440064e{-6}$	0.0116
	0.0500	$7.41110224e{-7}$	1.9739	$5.22978938e{-7}$	0.0201
	0.0250	$2.06592730e{-7}$	1.8429	$1.45787242e{-7}$	0.0357
	0.0125	$6.03562739e{-8}$	1.7752	$4.25922374e{-8}$	0.0639
	0.0063	$1.82739675e{-8}$	1.7237	$1.28957005e{-8}$	0.1237

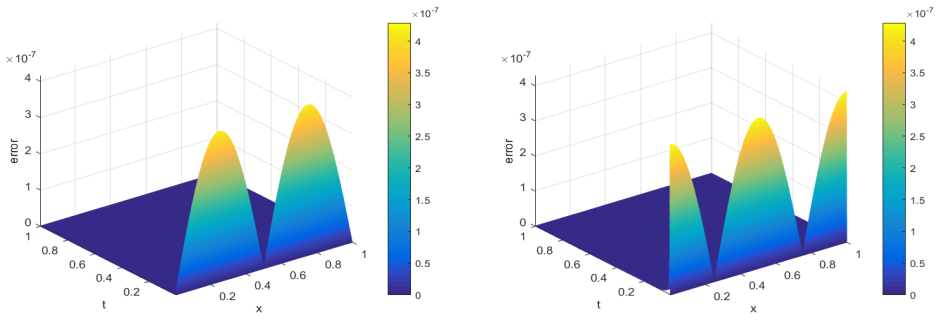


FIGURE 3. Error for ϕ (left) and ψ (right) with $\alpha = 0.05, N = 512$ and $dt = 0.002$ in Example 1.

TABLE 3. The obtained results for ϕ with a time step of $dt = 0.01$ in Example 2.

α	N	E_∞	$Ratio$	E_{RMS}	$CPU(s)$
0.05	256	$6.32111546e{-6}$	–	$3.62214720e{-6}$	0.4485
	512	$1.58281561e{-6}$	1.9961	$1.28136447e{-6}$	0.4862
	1024	$3.97132468e{-7}$	1.9853	$3.54102947e{-7}$	0.8807
	2048	$1.00573886e{-7}$	1.9428	$1.00082705e{-7}$	1.5812
0.1	256	$6.29181354e{-6}$	–	$3.60021790e{-6}$	0.3450
	512	$1.57732730e{-6}$	1.9883	$1.27463599e{-6}$	0.4817
	1024	$3.97597546e{-7}$	1.9548	$2.53263659e{-7}$	0.8517
	2048	$1.02527309e{-7}$	1.8323	$1.00556537e{-7}$	1.5848
0.2	256	$6.23901320e{-6}$	–	$3.55869996e{-6}$	0.2960
	512	$1.57089325e{-6}$	1.9488	$1.26361019e{-6}$	0.4784
	1024	$4.02755042e{-7}$	1.8122	$3.55331218e{-7}$	0.8492
	2048	$1.10582691e{-7}$	1.4265	$1.07733105e{-7}$	1.5675

describes the production or consumption rate of substance ϕ, measured in the same units of mol/(L·s). Furthermore, the diffusion coefficient $\lambda_3 = 0.002$, measured in square centimeters per second (cm^2/s), indicates how rapidly substances ψ and ϕ diffuse throughout their environment. Also we choose $f_1(x,t)$ and $f_2(x,t)$ so that the exact solutions of the above problem are as follows:

$$\phi(x,t) = t^{n-1}E_{m,n-1}(t^m)e^{\sin(2\pi x)}, \psi(x,t) = t^{n-1}E_{m,n-1}(t^m)e^{\cos(2\pi x)}.$$

Here $E_{m,n}(t)$ is Mittag-Leffler function.

Tables 5 and 6 detail the convergence rates, RMS errors, infinity norm errors, and CPU times for the functions ϕ and ψ across $0 \leq \alpha \leq 1$ with $N = 16$ and various time steps. The analysis shows that the convergence rates of the proposed method are nearing 2 in this range. Figure 6 shows the errors for ϕ and ψ at $N = 128$, $\alpha = 0.9$, and $dt = 0.002$.

TABLE 4. The obtained results for ψ with a time step of $dt = 0.01$ in Example 2.

α	N	E_∞	$Ratio$	E_{RMS}	$CPU(s)$
0.05	256	$3.23055897e{-6}$	–	$2.41374049e{-6}$	0.4560
	512	$8.09802531e{-7}$	1.9961	$7.54510342e{-7}$	0.4798
	1024	$2.04524961e{-7}$	1.9853	$2.03588440e{-7}$	0.8673
	2048	$5.3200041e{-8}$	1.9428	$4.09611940e{-8}$	1.5709
0.1	256	$3.14839887e{-6}$	–	$2.37040933e{-6}$	0.3020
	512	$7.93501368e{-7}$	1.9883	$7.41227078e{-7}$	0.4768
	1024	$2.04690246e{-7}$	1.9548	$2.02066680e{-7}$	0.8629
	2048	$5.74820452e{-8}$	1.8323	$4.15070419e{-8}$	1.5555
0.2	256	$2.98353570e{-6}$	–	$2.22887552e{-6}$	0.2949
	512	$7.72825001e{-7}$	1.9488	$7.01982701e{-7}$	0.4777
	1024	$2.20064291e{-7}$	1.8122	$2.08683310e{-7}$	0.8530
	2048	$8.18689248e{-8}$	1.4265	$7.64620800e{-8}$	1.5660

TABLE 5. The obtained results for ϕ using the proposed method when $N = 16$ in Example 3.

α	dt	E_∞	$C-R$	E_{RMS}	$CPU(s)$
0.7	0.0100	$8.99389937e{-6}$	–	$4.61487619e{-6}$	0.9984
	0.0050	$1.92354191e{-6}$	2.2252	$9.53524054e{-7}$	1.9599
	0.0025	$5.81071455e{-7}$	1.7270	$2.74005692e{-7}$	4.2684
0.8	0.0100	$1.89264678e{-5}$	–	$9.60103736e{-6}$	0.9732
	0.0050	$3.98758350e{-6}$	2.2468	$2.09132133e{-6}$	1.9948
	0.0025	$1.03323257e{-6}$	1.9483	$4.86620017e{-7}$	4.1974
0.9	0.0100	$3.88691997e{-5}$	–	$1.97795002e{-5}$	0.9547
	0.0050	$8.90377104e{-6}$	2.1261	$4.60807020e{-6}$	1.9444
	0.0025	$2.14469164e{-7}$	2.0536	$1.08508572e{-6}$	4.2914

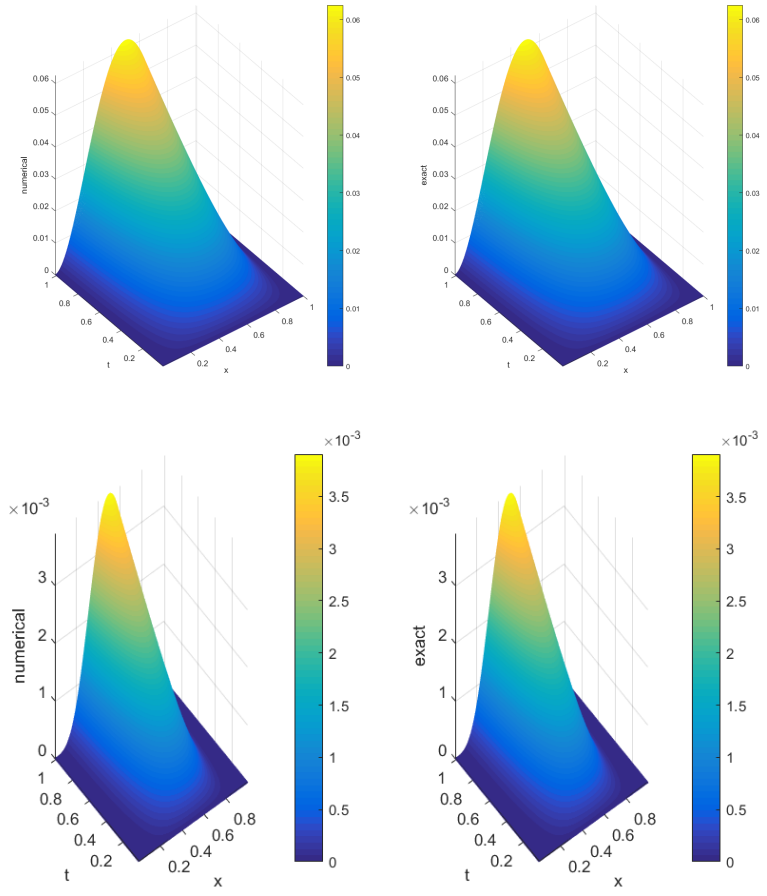


FIGURE 4. Exact and numerical solutions for ϕ (up) ψ (down) with $\alpha = 0.5, dt = 0.01$ and $N = 1024$ in Example 2.

5. **Concluding Remarks**

This research paper introduces a reliable numerical approach to solve the TFRDBS using a Caputo derivative of order $0 < \alpha < 1$. Spatial discretization of the problem was accomplished using the Fourier spectral method, ensuring efficiency and accuracy in our analysis. Further, a high-order approximation for the Caputo derivative, boasting a convergence order of $4-\alpha$, was utilized to tackle this system. Moreover, the convergence of this method has been validated as 2, as evidenced by the results of a numerical experiment. These findings illustrated consistent convergence rates of 2 across various values of α. Consequently, it was deduced that the method stands as an effective tool for resolving established systems.

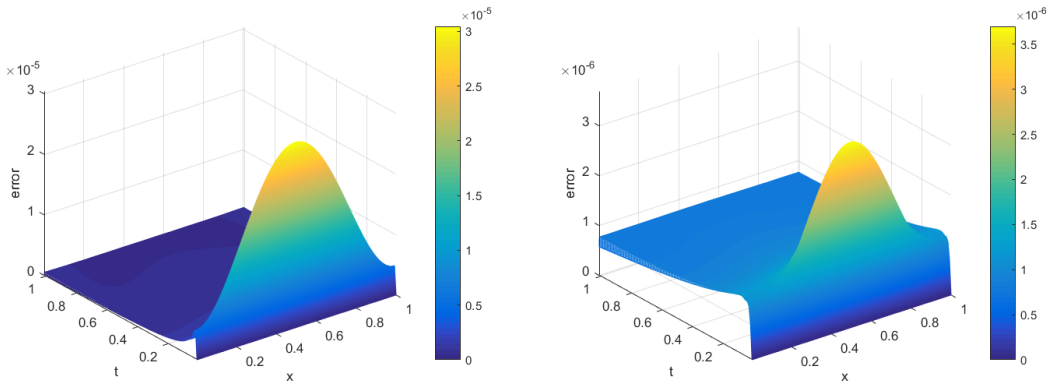


FIGURE 5. Error for ϕ (left) ψ (right) with $\alpha = 0.5, dt = 0.01$ and $N = 1024$ on $[0,1] \times [0,1]$ in Example 2.

TABLE 6. The obtained results for ψ using the proposed method when $N = 16$ in Example 3.

α	dt	E_∞	$C-R$	E_{RMS}	$CPU(s)$
0.7	0.0100	$1.71358254e{-5}$	–	$9.80544420e{-6}$	1.0351
	0.0050	$3.64434451e{-6}$	2.2333	$2.00038146e{-6}$	1.9890
	0.0025	$9.08167921e{-7}$	2.0046	$4.56865421e{-7}$	3.9809
0.8	0.0100	$3.73326760e{-5}$	–	$2.15622351e{-5}$	1.0177
	0.0050	$8.27073878e{-6}$	2.1744	$4.69353672e{-6}$	1.9385
	0.0025	$1.95168714e{-6}$	2.0833	$1.03892357e{-6}$	3.9796
0.9	0.0100	$7.92261077e{-5}$	–	$4.60146691e{-5}$	0.9534
	0.0050	$1.86063840e{-5}$	2.0902	$1.07301029e{-5}$	1.9356
	0.0025	$4.47500981e{-6}$	2.0558	$2.50829460e{-6}$	1.9356

Acknowledgments

I would also like express my gratitude to the meticulous referees for carefully reading this article.

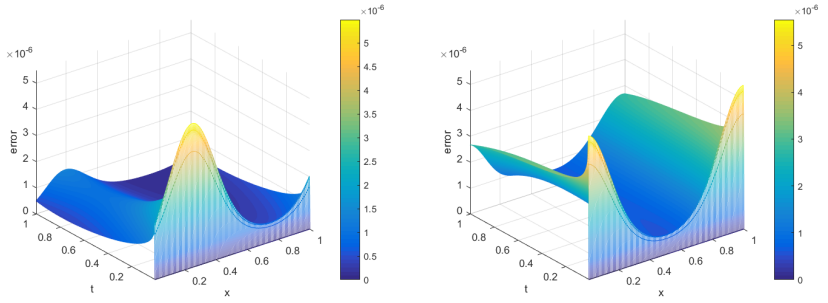


FIGURE 6. Error for ϕ (left) ψ (right) with $\alpha = 0.9, dt = 0.002$ and $N = 128$ on $[0,1] \times [0,1]$ in Example 3.

REFERENCES

[1] Al-deiakeh, R., Al-Smadi, M., Yusuf, A., Al-Omari, S. and Momani, S., 2023. Explicit solutions for fractional Chaffee–Infante reaction–diffusion coupled hierarchy system with conservation laws. *Mathematical Methods in the Applied Sciences*, *46*(12), pp.12777–12793. doi:10.1002/mma.9211

[2] Alabedalhadi, M., Al-Omari, S., Al-Smadi, M., Momani, S. and Suthar, D.L., 2023. New chirp soliton solutions for the space–time fractional perturbed Gerdjikov–Ivanov equation with conformable derivative. *Applied Mathematics in Science and Engineering*, *32*(1), p.2292175. doi:10.1080/27690911.2023.2292175

[3] Marom, O. and Momoniat, E., 2009. A comparison of numerical solutions of fractional diffusion models in finance. *Nonlinear Analysis: Real World Applications*, *10*(6), pp.3435–3442. doi:10.1016/j.nonrwa.2008.10.066

[4] Freeborn, T.J., 2013. A survey of fractional–order circuit models for biology and biomedicine. *IEEE Journal on Emerging and Selected Topics in Circuits and Systems*, *3*(3), pp.416–424. doi:10.1109/JETCAS.2013.2265797

[5] Neu, J.L., Prather, M.J. and Penner, J.E., 2007. Global atmospheric chemistry: Integrating over fractional cloud cover. *Journal of Geophysical Research*, *112*(D11), pp.1–12. doi:10.1029/2006JD008007

[6] Bai, J. and Feng, X., 2007. Fractional–order anisotropic diffusion for image denoising. *IEEE Transactions on Image Processing*, *16*(10), pp.2492–2502. doi:10.1109/TIP.2007.904971

[7] Iaffaldano, G., Caputo, M. and Martino, S., 2006. Experimental and theoretical memory diffusion of water in sand. *Hydrology and Earth System Sciences*, *10*(1), pp.93–100. doi:10.5194/hess-10-93-2006

[8] Raberto, M., Scalas, E. and Mainardi, F., 2002. Waiting–times and returns in high–frequency financial data: an empirical study. *Physica D: Nonlinear Phenomena*, *314*(1–4), pp.749–755. doi:10.1016/S0378-4371(02)01048-8

[9] Meng, Q.–J., Ding, D. and Sheng, Q., 2014. Preconditioned iterative methods for fractional diffusion models in finance. *Numerical Methods for Partial Differential Equations*, *31*(5), pp.1382–1395. doi:10.1002/num.21948

[10] Taylor, C.A., Fonte, T.A. and Min, J.K., 2013. Computational fluid dynamics applied to cardiac computed tomography for noninvasive quantification of fractional flow reserve. *Journal of the American College of Cardiology*, *61*(22), pp.2233–2241. doi:10.1016/j.jacc.2012.11.083

[11] Atangana, A., 2017. Fractal–fractional differentiation and integration: connecting fractal calculus and fractional calculus to predict complex system. *Chaos, Solitons & Fractals*, *102*, pp.396–406. doi:10.1016/j.chaos.2017.04.027

[12] Yang, F., Mou, J., Liu, J., Ma, C. and Yan, H., 2020. Characteristic analysis of the fractional–order hyperchaotic complex system and its image encryption application. *Signal Processing*, *169*, p.107373. doi:10.1016/j.sigpro.2019.107373

[13] Mittal, R.C. and Jiwari, R., 2011. Numerical solution of two–dimensional reaction–diffusion Brusselator system. *Applied Mathematics and Computation*, *217*(12), pp.5404–5415. doi:10.1016/j.amc.2010.12.010

[14] Siraj–ul–Islam, Ali, A. and Haq, S., 2010. A computational modeling of the behavior of the two–dimensional reaction–diffusion Brusselator system. *Applied Mathematical Modelling*, *34*(12), pp.3896–3909. doi:10.1016/j.apm.2010.03.028

[15] Jena, R.M., Rezazadeh, H. and Ganji, D.D., 2020. On the solution of time–fractional dynamical model of Brusselator reaction–diffusion system arising in chemical reactions. *Mathematical Methods in the Applied Sciences*, *43*(7), pp.3903–3913. doi:10.1002/mma.6141

[16] Jena, R.M., Rezazadeh, H. and Ganji, D.D., 2020. On the solution of time–fractional dynamical model of Brusselator reaction–diffusion system arising in chemical reactions. *Mathematical Methods in the Applied Sciences*, *43*(7), pp.3903–3913. doi:10.1002/mma.6141

[17] Singh, J., Rashidi, M.M., Kumar, D. and Swroop, R., 2016. A fractional model of a dynamical Brusselator reaction–diffusion system arising in triple collision and enzymatic reactions. *Nonlinear Engineering*, *5*(4), pp.277–285. doi:10.1515/nleng-2016-0041

[18] Nisar, K.S., Jagatheeshwari, R., Ravichandran, C. and Veeresha, P., 2023. An effective analytical method for fractional Brusselator reaction–diffusion system. *Mathematical Methods in the Applied Sciences*, *46*(18), pp.18749–18758. doi:10.1002/mma.9589

[19] Singh, M., Das, S. and Rajeev, N., 2024. An innovative Vieta–Fibonacci wavelet collocation method for the numerical solution of three–component Brusselator reaction–diffusion system of fractional order. *Journal of Mathematical Chemistry*, *62*(7), pp.1558–1594. doi:

[20] Boyd, J.P., 2013. *Chebyshev and Fourier Spectral Methods*. Springer. doi:

[21] Zaky, M.A., Babatin, M., Hammad, M., Akgül, A. and Hendy, A.S., 2024. Efficient spectral collocation method for nonlinear systems of fractional pantograph delay differential equations. *AIMS Mathematics*, *9*(6), pp.15246–15262. doi:10.3934/math.2024740

[22] Talaei, Y., Zaky, M.A. and Hendy, A.S., 2024. An easy–to–implement recursive fractional spectral–Galerkin method for multi–term weakly singular Volterra integral equations with non–smooth solutions. *Numerical Algorithms*, *97*, pp.1089–1117. doi:10.1007/s11075-023-01742-3

[23] Hendy, A.S., Qiao, L., Aldraiweesh, A. and Zaky, M.A., 2024. Optimal spectral Galerkin approximation for time and space fractional reaction–diffusion equations. *Applied Numerical Mathematics*, *201*, pp.118–128. doi:10.1016/j.apnum.2024.02.013

[24] Youssri, H.H., Zaky, M.A. and Hafez, R.M., 2024. Romanovski–Jacobi spectral schemes for high–order differential equations. *Applied Numerical Mathematics*, *198*, pp.148–159. doi:10.1016/j.apnum.2023.12.015

[25] Mohammadi, S., Fardi, M. and Ghasemi, M., 2023. A numerical investigation with energy–preservation for nonlinear space–fractional Klein–Gordon–Schrödinger system. *Computational & Applied Mathematics*, *42*(8), pp.1–27. doi:10.1007/s40314-023-02495-4

[26] Mohammadi, S., Ghasemi, M. and Fardi, M., 2022. A fast Fourier spectral exponential time–differencing method for solving the time–fractional mobile–immobile advection–dispersion equation. *Computational & Applied Mathematics*, *41*(6), pp.1–26. doi:10.1007/s40314-022-01970-8

[27] Mokhtari, R. and Mostajeran, F., 2019. A high–order formula to approximate the Caputo fractional derivative. *Communications on Applied Mathematics and Computation*, *2*(1), pp.1–29. doi:10.1007/s42967-019-00023-y

[28] Shen, J., Tang, T. and Wang, L.–L., 2011. *Spectral Methods*. Springer Science & Business Media.

Farzaneh Razavi Sosan
Department of Mathematics,
Faculty of Mathematical Sciences,
Shahrekord University,
Shahrekord 88186-34141, Iran.
Email: m.fardi@sku.ac.ir

Mehdi Ghasemi
Department of Mathematics,
Faculty of Mathematical Sciences,
Shahrekord University,
Shahrekord 88186-34141, Iran.
Email: mehd.ghasemi@gmail.com

Mojtaba Fardi
Department of Mathematics,
Faculty of Mathematical Sciences,
Shahrekord University,
Shahrekord 88186-34141, Iran.
Email: mojtaba.fardi@gmail.com



©2024 Shahid Chamran University of Ahvaz, Ahvaz, Iran. This article is an open-access article distributed under the terms and conditions of the Creative Commons Attribution-NonComertial 4.0 International (CC BY-NC 4.0 license) (http://creativecommons.org/licenses/by-nc/4.0/).